Revisiting the realization of artificial graphene in C_{60}/Cu(111)

D. Marchenko,[1,*,†] M. Krivenkov,[1,*] M. Sajedi,[1] A. Fedorov,[1,2,3] O. Rader,[1] and A. Varykhalov[1]
[1]*Helmholtz-Zentrum Berlin für Materialien und Energie, BESSY II, Albert-Einstein-Str. 15, 12489 Berlin, Germany*
[2]*IFW Dresden, Helmholtzstr. 20, 01069 Dresden, Germany*
[3]*Joint Laboratory 'Functional Quantum Materials' at BESSY II, 12489 Berlin, Germany*

(Received 24 January 2023; revised 14 July 2023; accepted 30 August 2023; published 26 September 2023)

Tamai *et al.* discovered an unusual electronic state near the Fermi level at the interface of Cu(111) and a molecular layer of C_{60}, which was initially attributed to C_{60}-Cu interfacial hybridization [Phys. Rev. B **77**, 075134 (2008)]. Later on, Yue *et al.* suggested that the state was due to the reshaping of a two-dimensional electron gas hosted at the Cu(111) surface, into an artificial graphene with Dirac cones by cutting out muffin-tin potentials of adsorbed fullerene molecules [Phys. Rev. B **102**, 201401(R) (2020)]. In the present paper, we introduce a different explanation using angle-resolved photoemission and show that the observed conical bands in the C_{60}/Cu(111) system are neither Dirac cones nor hybridization states. Rather, they are formed by *umklapp* scattering of photoelectrons emitted from bulk and surface bands of Cu(111) and diffracted on the (4×4) fullerene superstructure. The circular contours near the Fermi level, which resemble the low-energy part of graphene Dirac cones, are a result of the backfolding of the bulk band of copper, while the triangular silhouettes observed at higher binding energies, which mimic the threefold symmetric higher-binding-energy part of graphene Dirac cones, are due to an *umklapp* effect governed by highly coherent photoelectron diffraction of steeply dispersing Cu(111) *sp*-type surface resonances. We also used density functional theory to study the behavior of the two-dimensional electron gas localized within the honeycomb net created by the electron-exclusive potentials of C_{60} and demonstrate doping above the Fermi level (*p* doping). The results show no presence of the electronic structure of artificial graphene in C_{60}/Cu(111).

DOI: 10.1103/PhysRevB.108.115155

I. INTRODUCTION

Artificial graphene is a promising synthetic material [1] that can exhibit a wide range of electronic, optical, and magnetic properties. Up to now, it has been created using ultracold atoms trapped in optical lattices [2–4] and in molecular networks [5]. It was also studied theoretically for photonic crystals [6,7]. Molecular superstructures in contact with a 2D electron gas (2DEG) at metallic surfaces are a simple and appealing tool for fabricating artificial graphene through lateral reshaping of the surface potential into a honeycomb net. This process allows for the creation of interfacial states with exotic properties, including topological ones [5,8,9]. For example, topological Dirac cones were formed within the surface band structure of Cu(111) by nanostructuring adsorbed molecules of CO into a molecular graphene lattice [5]. Highly polar molecules of carbon monoxide, arranged in a hexagonal structure, create muffin-tin spheres of electron exclusion in the surface potential, which condense the 2DEG of Cu into a honeycomb-equivalent mesh and force electrons at the CO-Cu(111) interface to behave as they do in graphene. This mechanism is illustrated in Fig. 1(e).

Yue *et al.*'s recent study [10] is significant in that it reports the creation of artificial graphene from a 2DEG on surfaces of Cu(111) and Au(111) using nonpolar fullerene molecules, which are chemically inert and can additionally act as a protective coating for metallic surfaces [10,11]. Using angle-resolved photoemission (ARPES), they observed Dirac-cone-like features at the corners of the mini-Brillouin zones (m-BZ) of a (4×4) fullerene superlattice on Cu(111), with spots of intensity localized at the Fermi energy (E_F) and exactly at the $\overline{\mathrm{K}}$ points of the m-BZ (referred to as $\overline{\mathrm{K}}_{\mathrm{m}}$) identified as Dirac points. Approximately circular contours seen in constant energy surfaces (CES) at higher binding energies (E_B) with linear dispersion $E(\mathbf{k}_{\parallel})$ were identified as Dirac cones. The absence of dispersion of these features with photon energy (i.e., with the $\mathbf{k}_{\perp}$ component of the electron momentum) indicated their 2D character, further supporting the interpretation of the findings in terms of artificial graphene [10].

It is important to note a previous study by Tamai *et al.*, which also used ARPES to investigate the band structure of C_{60}/Cu(111) [12]. The data presented in that paper is similar to that of Ref. [10], but the authors explain the observed features in terms of a topologically trivial hybridization between C_{60} and the Cu(111) substrate. The study shows a Fermi surface with intensity spots at the corners of the fullerene m-BZ, accompanied by threefold symmetric Dirac-cone-like contours in the CES at higher E_B. These contours resemble the composition of crossing straight double lines. Although the authors indirectly supported their claim using density functional theory (DFT) calculations of total DOS and charge distribution, they did not present a full theoretical band structure that reproduces this hybridization state and reveals its *ab initio* $E(\mathbf{k})$ dispersion [12].

*These authors contributed equally to this work.
†Corresponding author: dmitry.marchenko@helmholtz-berlin.de

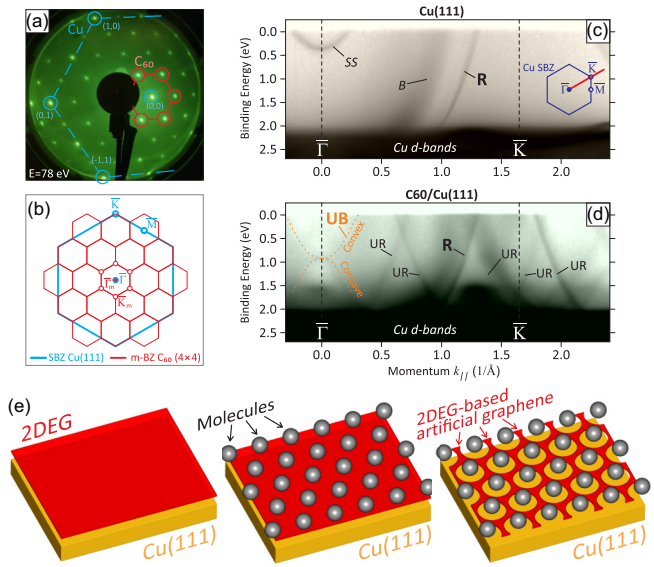

FIG. 1. Sample characterization and concept of artificial graphene formation. (a) Low-energy electron diffraction (LEED) pattern of molecular layer of C_{60} on Cu(111). Spots from Cu(111) are marked with blue circles/lines. C_{60}-derived 4×4 superstructure is marked in red. (b) Sketch showing surface Brillouin zone (SBZ) of Cu(111) (blue) and molecular *mini*-Brillouin zone (m-BZ) (red). [(c),(d)] Band structure of bare Cu(111) measured at $h\nu = 100$ eV along the $\overline{\Gamma} - \overline{\mathrm{K}}$ direction of the copper SBZ before and after deposition of C_{60}. In panel (d), one can observe the spectral feature UB (orange label), associated earlier with C_{60}-Cu hybridization [12], and cone-mimicking features UR (black labels) that arise from the *umklapp* replication of the copper band *R* along the $\mathbf{k}_{\parallel}$ [13]. (e) Schematic representation of the formation of electronic artificial graphene from the 2DEG at Cu(111). The hexagonal arrangement of C_{60} molecules imposes a periodic potential landscape that extrudes charge density from the surface and organizes the 2D electron gas into a honeycomb structure resembling graphene.

In the present study, we reexamine the electronic structure of C_{60}/Cu(111) using ARPES and revisit the explanations presented in two earlier reports [10,12]. We find that the bands observed in ARPES can neither be attributed to a hybridization state nor a Dirac cone. Instead, we show that the observed Dirac-cone-like features [10] are formed by *umklapp* scattering of photoelectrons emitted from various Cu bands and undergoing diffraction at the (4×4) molecular superstructure of C_{60} in the *final state* of the photoemission process. They result from a superposition of *umklapp*-generated spectroscopic features of *two different* types. The first type of features, which resemble the low-binding-energy part of a Dirac cone near the Fermi level, are created by a backfolding of the saddle-shaped bulk band of Cu from six $\overline{\mathrm{M}}$ points of the Cu(111) surface Brillouin zone to the $\overline{\Gamma}$ point, mediated by the lateral potential of the C_{60} superstructure [Fig. 3(b), see below]. This results in an ensemble of photoelectron intensity around $\overline{\Gamma}$ that effectively simulates six Dirac cones. This superposition was previously identified as Dirac cones of artificial graphene in Ref. [10] and as a hybridization state in Ref. [12]. The second type of relevant features occurs in the form of pronounced linearly dispersing bands with threefold symmetric, nearly triangular, isoenergetic contours in the CES, also centered at $\overline{\mathrm{K}}_{\mathrm{m}}$ points of the mini-Brillouin zone. It predominantly evolves further away from the Fermi level and perfectly resembles the trigonally warped high-binding-energy part of Dirac cones. In Ref. [12], these features were observed in CES as double lines and were also assigned to the hybridization state. Here, we show that they are also generated by the *umklapp* effect. Such patterns are created by a trivial replica of steeply dispersing *sp*-type surface resonances of Cu(111) [13] (often referred to as *sp*-bulk bands) caused by diffraction of photoelectrons at the (4×4) superstructure of C_{60}.

In addition, using density functional theory (DFT), we examine the actual response of the 2DEG on the Cu(111) surface after C_{60} deposition. Our calculations demonstrate that the molecular potentials cause the electron density to protrude from the copper surface, resulting in a honeycomb-shaped pattern of 2DEG localization. However, the 2DEG band is *p* doped above the Fermi level, inaccessible for photoemission, and does not resemble Dirac cone.

II. RESULTS AND DISCUSSION

A. Structure of C_{60}/Cu(111)

Structural characterization of the C_{60}/Cu(111) sample by low-energy electron diffraction (LEED) is reported in Fig. 1. Figure 1(a) shows LEED of Cu(111) deposited with one molecular layer (ML) of fullerenes. Diffraction spots originating from Cu(111) are marked with blue circles. One sees the formation of a sharp (4×4) molecular superstructure of C_{60}. Figure 1(b) displays interrelation between the Cu(111) surface Brillouin zone (label SBZ, shown in blue) and the molecular *mini*-Brillouin zone of the fullerene superstructure (label m-BZ, shown in red).

B. Composition of the false Dirac cones near the Fermi level

The electronic structure of Cu(111) undergoes significant changes when C_{60} is deposited, as evidenced by slices of the band structure along the direction $\overline{\Gamma} - \overline{\mathrm{K}}$ of the Cu(111) SBZ shown in Figs. 1(c) and 1(d) for the bare and C_{60}-deposited copper, respectively. The focus is on the binding-energy window between the Fermi level and $E_B \sim 2.1$ eV since higher binding energies are dominated by photoemission intensity from Cu *3d* bands, which are not of interest. Figure 1(c) shows characteristic features of the (111) faces of noble metals, such as a prominent Shockley-type surface state (labelled as SS) at the $\overline{\Gamma}$ point [14–16], the bulk *sp* band of copper (labelled as B), as well as an *sp*-type surface resonance (labelled as R) residing at the edge of the surface projection of the bulk *sp* band for the bare sample [13].

Upon deposition of fullerenes, the band structure of Cu(111) undergoes a substantial change, as shown in Fig. 1(d). The surface state SS quenches, and instead, a new faint state (labelled as UB) appears at the $\overline{\Gamma}$ point. The abbreviation UB stands for *umklapp*/bulk, as explained below. This state is better observed at lower photon energies ($h\nu < 40$ eV) in Fig. 2(d). It consists of a pair of convex/concave bands with positive/negative effective mass touching each other at $E_B = 0.93$ eV, forming a piece of intensity at the junction with locally flat dispersion [indicated by red arrows in Fig. 2(d)].

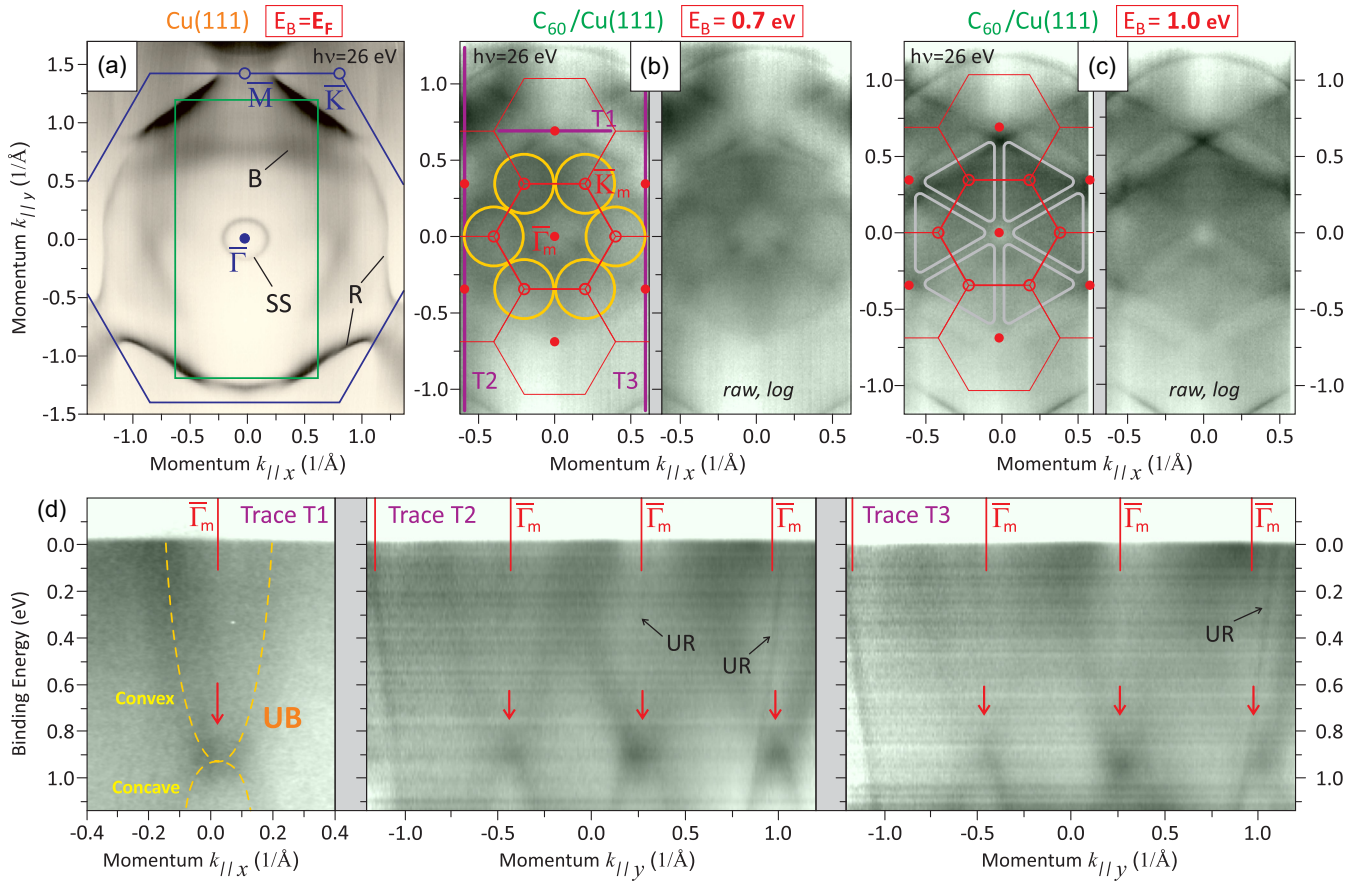

FIG. 2. *Umklapp* effects in photoemission from C_{60}/Cu(111) creating false Dirac cones near the Fermi energy. (a) Fermi surface of bare Cu(111) for reference. [(b),(c)] Constant energy surfaces (CES) sampled after deposition of C_{60} within an area marked in green in (a). (b) CES of C_{60}/Cu(111) acquired for $E_B = 0.7$ eV shows faint hexagonally arranged Dirac-cone-like contours [orange circles] centered at $\overline{K}_m$ of m-BZ. Right panel displays raw CES, left panel shows CES with auxiliary labels. (c) CES of C_{60}/Cu(111) measured for $E_B = 1.0$ eV reveals a net of threefold symmetric contours [gray triangles] also centered at $\overline{K}_m$. (d) Slices of the band structure of C_{60}/Cu(111) along lines T_1, T_2, and T_3 [as denoted in (b)] reveal that observed conical bands at low E_B belong to the spectral feature UB centered at $\overline{\Gamma}_m$ and recurring periodically in each m-BZ.

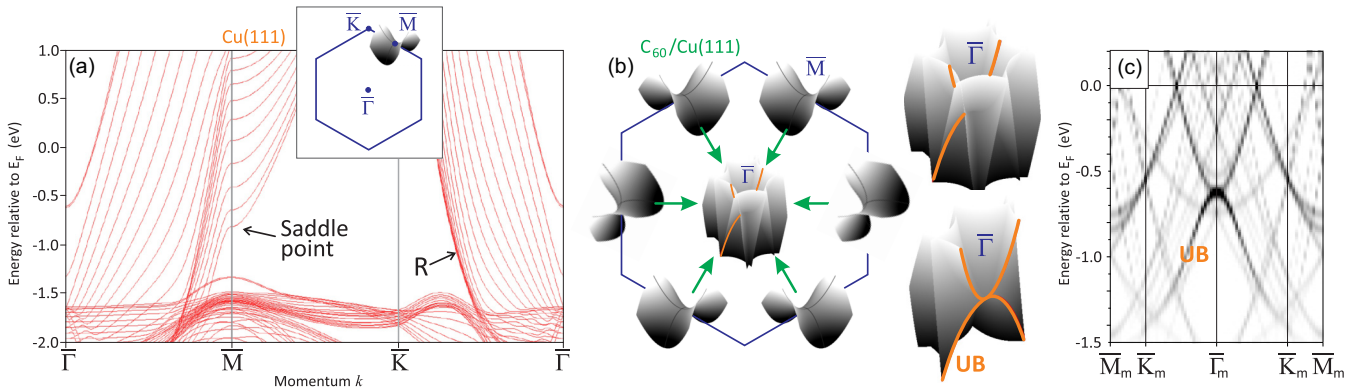

FIG. 3. Analysis by DFT of the feature UB. (a) DFT band structure of 20 layers Cu reveals a bulk saddle band at $\overline{M}$ of the Cu(111) SBZ. (b) Translation of six saddle bands from $\overline{M}$ to $\overline{\Gamma}$, caused by *umklapp* at the (4×4) superstructure of C_{60}, creates a band-shape arrangement around $\overline{\Gamma}$ which is the UB feature with convex (electron-like) and concave (hole-like) dispersions. (c) DFT calculation of a six-layer slab of bare Cu(111) with (4×4) supercell structure without unfolding. Here, the projection on *p* orbitals of two inner (i.e., bulk) copper layers is shown. It reproduces the feature UB without fullerene molecules and demonstrates that it is a combination of bulk band replicas.

UB is exactly the state observed earlier by Tamai *et al.*, which they attributed to the interfacial hybridization between C_{60} and Cu(111) [12].

Upon deposition of C_{60}, apart from the feature UB, a periodic set of seemingly conical bands (labelled UR, standing for *umklapp*/resonance) occurs, which could be misunderstood as Dirac cones. These bands occur periodically in registry to the m-BZ of the fullerene superlattice. However, upon closer inspection, it becomes clear that the dispersion of these bands precisely reproduces the dispersion of the *sp*-type surface resonance R seen in bare Cu(111) [Fig. 1(c)]. Further examination reveals that all UR bands are just replicas of the steeply-dispersing band R, sampled for both directions of electron momentum $-\mathbf{k}$ and $+\mathbf{k}$ and repeated along the momentum axis with periodicity of the m-BZ.

The reason for the observed replication of the R band is the *umklapp* scattering of the photoelectrons on the adsorbed molecular network. This is exactly the same mechanism that we found to be responsible for the occurrence of false Dirac cones in C_{60}/Au(111) in an earlier study [13]. In the following, we will explain in detail how the interplay between the *umklapp* replicas UR of the copper surface resonance and the feature UB, created by *umklapp* of the copper bulk band, results in the falsification of Dirac cones of artificial graphene in photoemission.

Shown in Fig. 2(b) is the CES of C_{60}/Cu(111) measured at $E_B = 0.7$ eV with low photon energy $h\nu = 26$ eV. By comparing it to the Fermi surface of bare Cu(111) [Fig. 2(a), where the Cu(111) SBZ is plotted with blue lines], the (4×4) m-BZ of the molecular superstructure (red hexagons) is identified. At the corners of the m-BZ (points $\overline{\mathrm{K}}_\mathrm{m}$), faint and blurry circular contours of photoemission intensity are observed, as depicted in the right panel of Fig. 2(b). The left panel of Fig. 2(b) shows the same data with auxiliary labels (circular contours are emphasized here by orange circles). These contours were previously identified as Dirac cones of artificial graphene in Ref. [10]. They are traceable in all CESs for binding energies from the Fermi level down to $E_B \sim 0.9$ eV and appear to scale up in momentum space with increasing E_B, which makes them look quite similar to Dirac cones. A closer examination of the overall connectivity of the band structure E(**k**) reveals that these circular contours are not Dirac cones but are instead a part of the spectral feature UB.

In Fig. 2(d), the band structure of C_{60}/Cu(111) is shown along lines T_1, T_2, and T_3, which are marked by bold magenta lines in Fig. 2(b). These traces pass through $\overline{\Gamma}_\mathrm{m}$, $\overline{\mathrm{M}}_\mathrm{m}$ and $\overline{\mathrm{K}}_\mathrm{m}$ points of neighboring m-BZs. In the left panel the dispersion of UB is outlined with dashed orange lines. Apparently linear (but actually massive) convex bands, forming circular contours of false Dirac cones in CES, start their dispersion towards E_F from the intense flat part of UB at $E_B \sim 0.9$ eV (red arrows). UB repeats periodically according to the (4×4) periodicity of C_{60} and reoccurs in the centers of every m-BZ (this period is emphasized by red vertical dashes corresponding to $\overline{\Gamma}_\mathrm{m}$). All copies of UB, forming cone-like features at $\overline{\mathrm{K}}$ points of the m-BZ, create a (4×4) net of convex bands.

To gain insight into the nature of band UB, one must examine the bulk electronic structure of Cu. The band dispersion along the high-symmetry directions $\overline{\Gamma}-\overline{\mathrm{M}}-\overline{\mathrm{K}}-\overline{\Gamma}$ of the Cu(111) SBZ was calculated using DFT, and the results are presented in Fig. 3(a). The bulk *sp* band has a saddle-shaped dispersion at the $\overline{\mathrm{M}}$ point. Because of the (4×4) superstructure of C_{60}, the six saddle points $\overline{\mathrm{M}}$ are backfolded to the center of the SBZ $\overline{\Gamma}$, as shown in Fig. 3(b). As a result, an ensemble of photoelectron intensity composed of a superposition of saddle-bands is created. These saddle-bands are azimuthally rotated relative to each other by 120° (around the normal direction to the crystal surface). The resulting pattern UB, as well as an exemplary section along the direction $\overline{\Gamma}-\overline{\mathrm{M}}$, is presented in the right panel of Fig. 3(b). The section qualitatively reproduces the experimentally observed dispersion of UB [Fig. 2(d)]. It is clear that convex and concave bands are formed by the saddles translated from different $\overline{\mathrm{M}}$ points and that the observed composition of UB is only possible due to the specific azimuthal orientation of the saddle bands in **k** space at different $\overline{\mathrm{M}}$ points. Furthermore, from general symmetry considerations, the *umklapp* process replicates this ensemble of superimposed saddle-bands to the $\overline{\Gamma}_\mathrm{m}$ points of every m-BZ, as seen in the experiment [Fig. 2(d)].

To verify the assertion that UB originates from the Cu bands, and to further support this claim, we conducted DFT calculations of a bare Cu(111) surface (six ML) in a (4×4) superstructure unit cell, without any C_{60} molecules present. The resulting band structure without unfolding is depicted in Fig. 3(c). The UB feature with convex and concave bands is clearly reproduced, and is shown to be a combination of *sp*-band replicas from different $\overline{\mathrm{M}}$ points. This serves as additional evidence that the observed UB in the C_{60}/Cu(111) system is indeed derived from the underlying Cu bands.

C. False Dirac cones with trigonal warping at higher binding energies

Reference [10] discussed (mimics of) Dirac cones near the Fermi level, but there are other remarkable spectral features resembling Dirac cones at higher binding energies. In CESs measured for $E_B > 0.9$ eV (below the junction energy of convex/concave bands of UB), the circular contours created by the bulk-band-derived *umklapp* UB vanish completely. Instead, pronounced threefold symmetric, almost triangular contours of a different type appear. Figure 2(c) shows a CES measured at $E_B = 1.0$ eV. The right panel shows the raw CES, while the left panel shows the CES with auxiliary labels and triangular contours emphasized by gray lines.

The origin of these triangular contours is straightforward. They are composed of straight lines formed by *umklapp* replication of the *sp*-type band of Cu(111) labeled as R in Fig. 1(c). Multiple replicas of R, labeled in Fig. 1(d) as UR, are exactly the bands that render this net of straight lines. The UR features are seen to a much better extent at higher photon energies $h\nu > 60$ eV.

The bottom panels of Fig. 4(a) show three CESs measured for $E_B = 0.1$ eV (nearly Fermi surface), $E_B = 0.7$ eV, and $E_B = 1.1$ eV from the C_{60}/Cu(111) sample using $h\nu = 100$ eV. The top panels of Fig. 4(a) report comparative data sets, acquired for the same energies but from bare Cu(111). The difference between CESs of bare and fullerene-covered Cu(111) is remarkable. While for Cu(111), a textbook-like Fermi surface and CESs composed of hexagonal contours

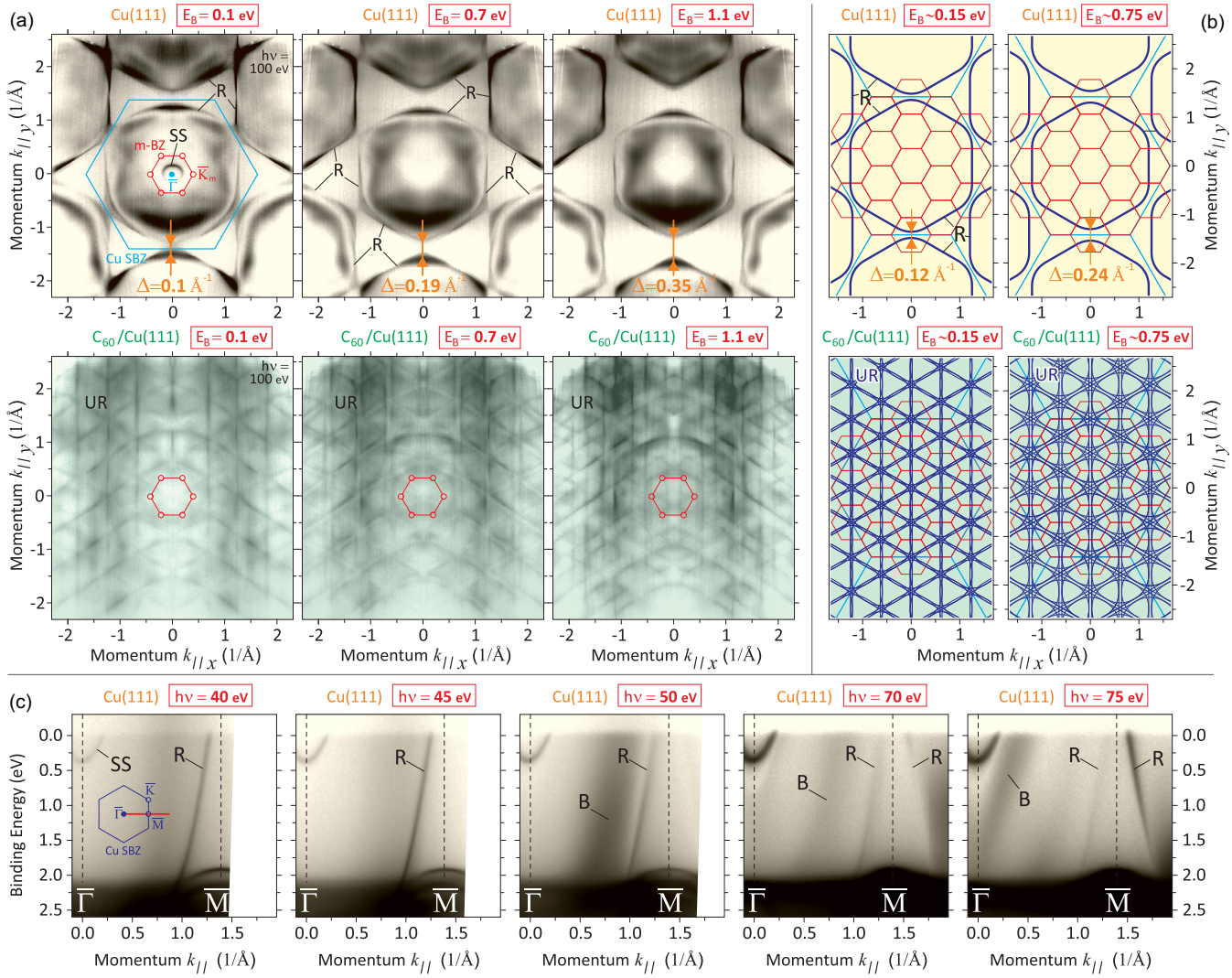

FIG. 4. *Umklapp* effects in C_{60}/Cu(111) that create trigonally warped contours of false Dirac cones at higher binding energies through the replication of Cu surface resonances. (a) CES measured for binding energies $E_B = 0.1$ eV, $E_B = 0.7$ eV, and $E_B = 1.1$ eV from bare Cu(111) (upper panels) and from C_{60}/Cu(111) (lower panels). Deposition of fullerenes creates a change in CES topology towards a net of single and double straight lines (pattern UR), which is created by multiple replication of the hexagonal-shaped copper band *R* according to the periodicity of the molecular m-BZ. SBZ of Cu(111) and m-BZ of C_{60} are marked by light-blue and red lines, respectively. (b) Geometric model of *umklapp* replication for CES corresponding to $E_B \sim 0.15$ eV and $E_B \sim 0.75$ eV, which shows the replication of contours *R* across each m-BZ entering into the first SBZ of Cu(111). The net-like topology of the CES pattern UR (single or double line) depends on the **k** separation Δ between Cu bands *R* from the first and second SBZs. (c) Band structure of bare Cu(111) measured at different photon energies, which reveals no dispersion of the Cu band *R* with $\mathbf{k}_\perp$, attesting to its surface-resonance-like 2D behavior [13].

of the copper *sp*-band R are observed, for fullerene-covered Cu(111), a perfectly periodic net of single or double straight lines is seen. This net is rendered by UR replicas of the copper band R, *umklapp* translated in **k** space according to the (4 × 4) periodicity of the molecular m-BZ.

Figure 4(b) reports a simple graphical simulation of such replication in CESs, performed for binding energies $E_B \sim 0.15$ eV and $E_B \sim 0.75$ eV. Upper panels show CESs of bare Cu(111). Hexagon-shaped Cu bands R (bold dark-blue line) are taken and replicated coherently over multiple m-BZs of C_{60} (red hexagons) in such a way that the $\overline{\Gamma}$ point of copper SBZ translates to the $\overline{\Gamma}_m$ point of every m-BZ. The resulting CESs are displayed in the bottom panels. One sees that the type of the generated pattern (single or double lines) depends on the size of the hexagonal isoenergetic contour of the band R compared to the size of the Cu(111) SBZ or, in other words, on the momentum separation between R bands from the first and second SBZ of copper. The magnitude of this separation is introduced in the top panels of Fig. 4(b) as parameter Δ at the $\overline{M}$ point of Cu.

Due to $E(\mathbf{k})$ dispersion of the R band, Δ is sensitive to the binding energy of the CES. For very small Δ close to zero (which corresponds to Fermi energy), the replication routine results in the net of UR replica organized in single (actually, overlapping double) lines. Upon increasing the binding energy and enlarging the separation Δ, single lines split into double and the distance between them sequentially increases with increasing E_B of the CES. Such a simple model of *umklapp*

replication accurately describes the experimental results. In our previous paper on C_{60} on Au(111), we reported a similar *umklapp* effect [13]. However, the *umklapp* net observed in that system was generated by a different molecular superstructure ($2\sqrt{3} \times 2\sqrt{3}\,R30^\circ$) and was less coherent to the Au(111) SBZ.

We want to emphasize that the observed *umklapp* net of the straight lines UR is also a diffraction-driven effect occurring in the final state of photoemission, similarly to the bulk-band *umklapp* UB. We provided arguments supporting this scenario, such as the absence of minigaps [17–19] at the crossings of R and UR, and the weak bonding and large separation between fullerenes and the surface of the noble metal, which we discussed in detail in Ref. [13] in the context of the C_{60}/Au(111) system. The spectral features UR have a remarkable property: neither the Dirac-cone-like bands formed by the replica UR of the copper band R in $E(\mathbf{k})$ dispersions [Fig. 1(d)], nor their triangular contours in CESs disperse upon variation of the photon energy $h\nu$ (equivalent to variation of perpendicular component of electron momentum $\mathbf{k}_\perp$).

The reason for this was revealed by our atomic-layer-resolved DFT analysis of Au(111) in Ref. [13], where we showed that the state R has a 2D-like character. Contrary to common belief that it represents a bulk *sp* band, the band R is not a pure bulk state. Instead, it can be considered as a deep surface resonance residing at the edge of the surface projection of the copper bulk *sp* band onto the (111) plane [see our DFT in Fig. 3(a), where this surface resonance is accurately reproduced along the line $\overline{\Gamma} - \overline{\mathrm{K}}$]. The surface resonance R leaks into the bulk but has no k_z dispersion.

The experimental $E(\mathbf{k}_\parallel)$ dispersions of the band R, measured along the direction $\overline{\Gamma} - \overline{\mathrm{K}}$ of the Cu(111) SBZ for varying photon energies $h\nu = 40 - 75\,\mathrm{eV}$, are shown in Fig. 4(c). The band does not change its binding energy upon a change in $h\nu$, while the $E(\mathbf{k}_\perp)$ dispersion of the real bulk *sp* band (label B) is clearly seen. As a result, the whole net of the replica UR, including triangular contours of the false Dirac cones in CESs, does not show any dispersion with $\mathbf{k}_\perp$ and behaves as 2D. Therefore, the dispersionless character of Dirac-cone-like features with photon energy cannot be used as proof of artificial graphene formed within a 2DEG, contrary to what is proposed in Ref. [10].

In conclusion, the replicas UR of band R are crucial in mimicking the Dirac cones in the C_{60}/Cu(111) system. At low binding energies ($E_B < 0.9\,\mathrm{eV}$), the false Dirac cones at $\overline{\mathrm{K}}_\mathrm{m}$ points of the molecular m-BZ are mimicked by the spectral feature UB, which is formed by the overlapping of *umklapp*-replicated saddle-shaped bulk bands of Cu. At higher binding energies, the *umklapp* replicas UR of the copper surface resonance R become the dominant factor. These replicas UR form nearly triangular contours, also centered at $\overline{\mathrm{K}}_\mathrm{m}$ and resembling the threefold warped isoenergetic contours of the π band of graphene.

Objectively, we cannot rule out the potential existence of an artificial Dirac cone dispersion that might not be observable in photoemission due to matrix element effects. We show that the bands, which are visible have an explanation based on periodic replication of copper bands resulting from photoemission final state scattering.

D. DFT analysis of 2DEG of Cu(111) with imposed molecular potentials

To confirm that the observed conical features in the C_{60}/Cu(111) system are not due to artificial graphene, we utilized *first-principles* DFT calculations to investigate the electronic interaction between C_{60} and Cu(111). Specifically, we examined the spatial localization of the two-dimensional electron gas (2DEG) at the Cu(111) surface with the fullerene superstructure deposited. The purpose was to determine if the muffin-tin potential of molecules causes the 2DEG to form a honeycomb superstructure and, if so, how the band structure E(**k**) of the reshaped 2DEG will be modified. It is a necessary precondition to have this kind of spatial localization for the formation of artificial graphene [5].

In the upper panel of Fig. 5(a), we illustrate the spatial localization of the charge density of the 2DEG at the Cu(111) surface, which is shown as yellow/green-colored layers. The thick charge layer of predominant localization is in vacuum and above the first atomic layer of Cu, while the second, thinner layer resides between the first and second atomic layers of Cu. The calculated band structure is marked in the bottom panel of Fig. 5(a) by a thick orange dot, corresponding to the presented 2DEG spatial localization. As expected, the band of 2DEG is the prominent Shockley-type surface state of Cu(111) [14–16], and its localization in the form of a dipole double layer fully corresponds with a solution of the Schrödinger equation for Bloch waves with a boundary condition of crystal termination [20,21], which describes nearly free-electron-like surface states.

Figures 5(b)–5(d) depict the changes in spatial localization (top panels) and band dispersion (bottom panels) of the 2DEG as the (4×4) superlattice of C_{60} is gradually brought closer to the Cu(111) surface, with the distance d between fullerenes and Cu(111) decreasing until the fully relaxed equilibrium configuration is reached ($d = 1.9$ Å) [Fig. 5(d)]. The distance d is defined as the distance between the bottom atoms of the fullerene cage and the first atomic layer of Cu. The results show that as the fullerenes approach the Cu(111) surface, the molecular potentials do indeed push the charge density of the 2DEG out of the molecular sites and laterally reshape the dipole bilayer into a honeycomb net, which is in qualitative agreement with the scenario proposed in Ref. [10] and sketched in Fig. 1(e). However, as the fullerenes come closer to Cu(111), the 2DEG moves towards lower binding energies due to strengthening of charge doping and ends up just above the Fermi level in the equilibrium configuration (and becomes inaccessible for photoemission).

III. SUMMARY

We used ARPES to study the electronic structure of a (4×4) superlattice of C_{60} fullerenes on the noble-metal surface Cu(111). This system exhibits a unique C_{60}-induced electronic state near the Fermi level as a pair of convex/concave bands touching at the binding energy $E_B = 0.9\,\mathrm{eV}$. The origin of this state was disputed, with Tamai *et al.* [12] attributing it to trivial C_{60}-Cu(111) interfacial hybridization, while Yue *et al.* [10] reported that the concave part forms conical bands and identified them as topological Dirac cones. They proposed

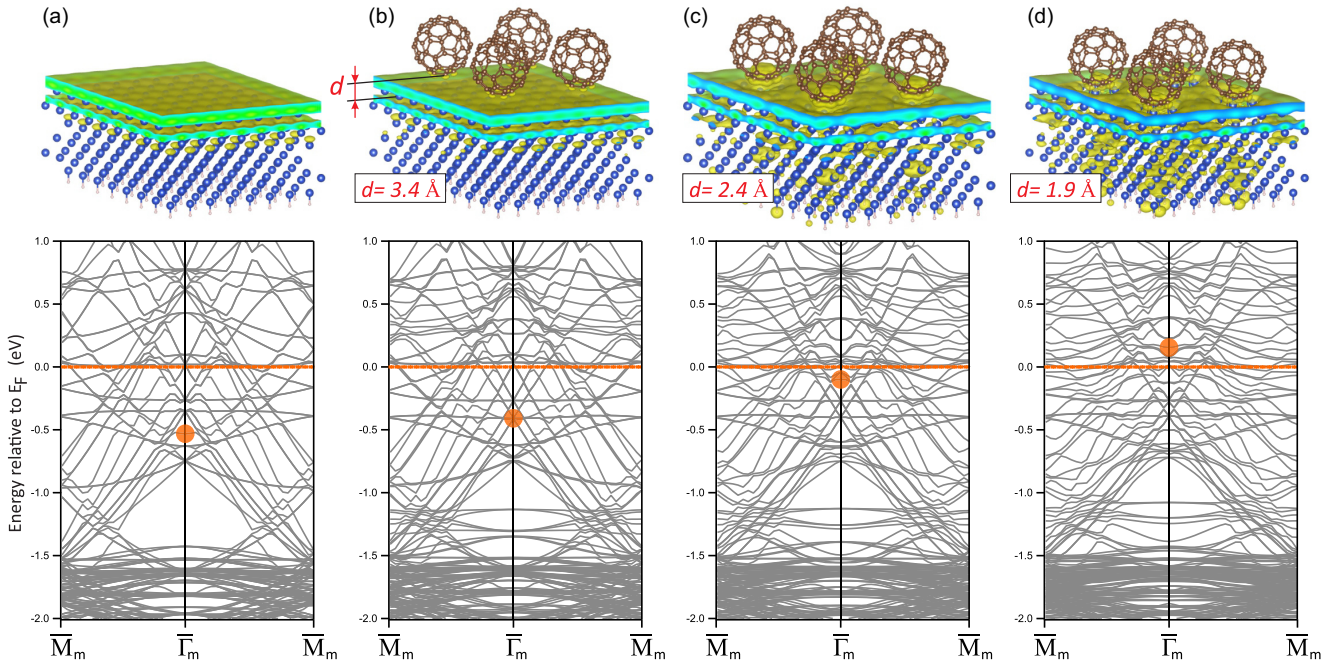

FIG. 5. Interaction of C_{60} with the 2DEG at the surface of Cu(111) studied by density functional theory (DFT). The top panels show the spatial localization of the dipole bilayer of 2DEG, with corresponding band structures below. The energy position of the 2DEG band (Shockley-type surface state) at the $\overline{\Gamma}_m$ point is emphasized with a thick orange dot. The calculations are presented for decreasing distance d between C_{60} and Cu(111): (a) bare Cu(111), (b) $d = 3.4$ Å, (c) $d = 2.4$ Å, (d) $d = 1.9$ Å (equilibrium separation). While the fullerene potentials extrude the 2DEG from the adsorption sites of C_{60} and reshape it into a honeycomb-like net, they also push the 2DEG band up in energy.

as reason for this the formation of an artificial graphene within the 2DEG of Cu(111) reshaped in a honeycomb net by protruding muffin-tin potentials of adsorbed molecules [10].

We conducted an extensive study of the electronic state in question using ARPES and found that it is *neither* of topological nature *nor* a trivial hybridization-induced state. It does not form Dirac cones, but only mimics them. We discovered that this state (UB) is created by a backfolding of bulk copper bands from six $\overline{M}$ points of the Cu(111) SBZ into the SBZ center $\overline{\Gamma}$, caused by *umklapp* of the photoelectrons on the (4×4) potential of the molecular superlattice. The bulk *sp* band has a saddle-shaped dispersion at the $\overline{M}$ points, which, when translationally copied to the SBZ center, creates a very specific superpositional ensemble of photoelectron intensity, rendering both convex and concave bands as well as false Dirac cones at the corners of molecular *mini*-BZs. We stress that the observed state UB is not a ground-state band but solely a final state effect of photoelectron diffraction.

At higher binding energies, we discovered a pronounced, perfectly coherent net of linear bands UR, also generated by *umklapp*, but this time by the diffraction of Cu(111) *sp*-type surface resonances. This net creates triangular silhouettes in constant energy surfaces, which strongly resemble threefold warped parts of Dirac cones away from the Dirac point. These higher-binding-energy triangular silhouettes UR and lower-binding-energy conical dispersions UB complement each other and make the mimicking of Dirac cones in the C_{60}/Cu(111) system perfect.

Our experiment was complemented by a DFT study of the 2DEG under the influence of the adsorbed fullerenes. We found evidence of the reshaping of the 2DEG dipole bilayer by electron-exclusive potentials of C_{60} towards a honeycomb-like configuration in the maps of charge localization. However, we observed only minor modifications of the 2DEG band structure, mainly an energy shift under preservation of the massive character.

We see no indications of artificial graphene in the C_{60}/Cu(111) system.

IV. METHODS

The sample of C_{60}/Cu(111) was prepared *in situ*. An atomically clean surface of Cu(111) was prepared through repeated cycles of Ar^+ sputtering at 1 kV and subsequent annealing at 800 K. Fullerenes were deposited from heated powder in a molybdenum crucible. Afterwards, the highly ordered (4×4) superstructure of C_{60} was achieved by short annealing of the sample at 600 K.

The band structure of C_{60}/Cu(111) was studied through ARPES at BESSY II using the endstation ARPES 1^2 installed at the beamline UE112-PGM2a and equipped with a Scienta R8000 hemispherical analyzer and the full-6-axes sample manipulator S6.Cryo [22]. We used variable energy and polarization of synchrotron light. The availability of variable photon energy ($h\nu$) was critically important to see the full picture of the band structure. The convex/concave band UB was observed practically only at low $h\nu$ (<40 eV), while *umklapp*-induced replicas of copper surface resonances *R* were detectable to much better extent at higher $h\nu$ (>60 eV) Photoemission measurements of all *umklapp* effects in C_{60}/Cu(111) were conducted at low sample temperatures T<20 K.

To analyze the structure, DFT calculations with structural optimization were performed using the VASP package [23] with the PAW method [24] in the PBE approximation [25]. Four types of structures were analysed in the present paper:

(i) DFT calculation of bare Cu(111) as 20 layers of copper in a 70-Å slab, using 11×11 Monkhorst-Pack grid [26] and 450 eV cutoff energy for the plane-wave-basis set. This calculation is conducted to demonstrate the general copper bulk bandstructure and the saddle point dispersion at $\overline{\mathrm{M}}$ [Fig. 3(a)].

(ii) DFT calculation of six layers bare Cu(111) (4×4) supercell in a 50 Å slab, without subsequent unfolding. A 5×5 Monkhorst-Pack grid [26] and 470 eV cutoff energy for the plane-wave-basis set were used. The backside was passivated by hydrogen atoms. Dipole correction, DFT-D2 [27] van der Waals interaction correction are included. The calculation demonstrates the formation of the feature UB as a combination of copper bulk band replica due to the supercell without fullerene molecules on top. It also allows to determine the spatial localization of the charge density of Cu(111) surface state (2DEG) [Figs. 3(c) and 5(a)].

(iii) DFT calculation of C_{60} on Cu(111) using six-atomic-layer-thick copper with parameters as in (ii). Fullerene molecules adsorbed at hollow sites with a hexagon ring facing the substrate [28,29]. We obtain a relaxed distance of $d = 1.9$ Å. The backside is passivated by hydrogen atoms. Analysis of the charge density of different bands at $\overline{\Gamma}$ allows to determine the 2DEG localization and shows that it is reshaped into the honeycomb net. The corresponding band moves, however, above the Fermi level [Fig. 5(d)].

(iv) DFT calculation of C_{60} on Cu(111) with the same parameters as above but with fullerene molecules positioned at larger distances from the copper surface. This allows to see the transition from the pure Cu(111) 2DEG to the honeycomb-net reshaped 2DEG of C_{60}/Cu(111) with the corresponding modification of the 2DEG energy [Figs. 5(b) and 5(c)].

ACKNOWLEDGMENTS

This work was supported by Impuls- und Vernetzungsfonds der Helmholtz-Gemeinschaft under Grant No. HRSF-0067.

Authors declare no competing interests.

[1] M. Polini, F. Guinea, M. Lewenstein, H. C. Manoharan, V. Pellegrini, Artificial honeycomb lattices for electrons, atoms and photons, Nat. Nanotechnol. **8**, 625 (2013).

[2] I. Bloch, Ultracold quantum gases in optical lattices, Nat. Phys. **1**, 23 (2005).

[3] B. Wunsch, F. Guinea, and F. Sols, Dirac-point engineering and topological phase transitions in honeycomb optical lattices, New J. Phys. **10**, 103027 (2008).

[4] S.-L. Zhu, B. Wang, L.-M. Duan, Simulation and Detection of Dirac Fermions with Cold Atoms in an Optical Lattice, Phys. Rev. Lett. **98**, 260402 (2007).

[5] K. K. Gomes, W. Mar, W. Ko, F. Guinea, and H. C. Manoharan, Designer Dirac fermions and topological phases in molecular graphene, Nat. Phys. **483**, 306 (2012).

[6] F. D. M. Haldane, S. Raghu, Possible Realization of Directional Optical Waveguides in Photonic Crystals with Broken Time-Reversal Symmetry, Phys. Rev. Lett. **100**, 013904 (2008).

[7] R. A. Sepkhanov, Yu. B. Bazaliy, C. W. J. Beenakker, Extremal transmission at the Dirac point of a photonic band structure, Phys. Rev. A **75**, 063813 (2007).

[8] Z. Liu, J. Wang, J. Li, Dirac cones in two-dimensional systems: From hexagonal to square lattices, Phys. Chem. Chem. Phys. **15**, 18855 (2013).

[9] C.-H. Park, S. G. Louie, Making Massless Dirac Fermions from a Patterned Two-Dimensional Electron Gas, Nano Lett. **9**, 1793 (2009).

[10] S. Yue, H. Zhou, D. Geng, Z. Sun, M. Arita, K. Shimada, P. Cheng, L. Chen, S. Meng, K. Wu, B. Feng, Experimental observation of Dirac cones in artificial graphene lattices, Phys. Rev. B **102**, 201401(R) (2020).

[11] K. M. Amin, H. M. A. Amin, (Eds.), *Corrosion Protection of Metals and Alloys Using Graphene and Biopolymer Based Nanocomposites*, (1st ed.) (CRC Press, Boca Raton, FL, 2021).

[12] A. Tamai, A. P. Seitsonen, F. Baumberger, M. Hengsberger, Z.-X. Shen, T. Greber, J. Osterwalder, Electronic structure at the C_{60}/metal interface: An angle-resolved photoemission and first-principles study, Phys. Rev. B **77**, 075134 (2008).

[13] M. Krivenkov, D. Marchenko, M. Sajedi, A. Fedorov, O. J. Clark, J. Sánchez-Barriga, E. D. L. Rienks, O. Rader, and A. Varykhalov, On the problem of Dirac cones in fullerenes on gold, Nanoscale **14**, 9124 (2022).

[14] S. D. Kevan, R. H. Gaylord, High-resolution photoemission study of the electronic structure of the noble-metal (111) surfaces, Phys. Rev. B **36**, 5809 (1987).

[15] F. Reinert, G. Nicolay, S. Schmidt, D. Ehm, S. Hüfner, Direct measurements of the L-gap surface states on the (111) face of noble metals by photoelectron spectroscopy, Phys. Rev. B **63**, 115415 (2001).

[16] A. Tamai, W. Meevasana, P. D. C. King, C. W. Nicholson, A. de la Torre, E. Rozbicki, F. Baumberger, Spin-orbit splitting of the Shockley surface state on Cu(111), Phys. Rev. B **87**, 075113 (2013).

[17] I. Pletikosić, M. Kralj, P. Pervan, R. Brako, J. Coraux, A. T. N'Diaye, C. Busse, T. Michely, Dirac Cones and Minigaps for Graphene on Ir(111), Phys. Rev. Lett. **102**, 056808 (2009).

[18] S. Rusponi, M. Papagno, P. Moras, S. Vlaic, M. Etzkorn, P. M. Sheverdyaeva, D. Pacilé, H. Brune, C. Carbone, Highly Anisotropic Dirac Cones in Epitaxial Graphene Modulated by an Island Superlattice, Phys. Rev. Lett. **105**, 246803 (2010).

[19] J. Sánchez-Barriga, A. Varykhalov, D. Marchenko, M. R. Scholz, O. Rader, Minigap isotropy and broken chirality in graphene with periodic corrugation enhanced by cluster superlattices, Phys. Rev. B **85**, 201413(R) (2012).

[20] W. Shockley, On the surface states associated with a periodic potential, Phys. Rev. **56**, 317 (1939).

[21] S. G. Davison, M. Stęślicka, *Basic Theory of Surface States* (Clarendon Press, London, 1992).

[22] www.arpes-robotics.com.

[23] G. Kresse, J. Hafner, *Ab initio* molecular dynamics for liquid metals, Phys. Rev. B **47**, 558 (1993).

[24] P. E. Blöchl, Projector augmented-wave method, Phys. Rev. B **50**, 17953 (1994).

[25] J. P. Perdew, K. Burke, and M. Ernzerhof, Generalized Gradient Approximation Made Simple, Phys. Rev. Lett. **77**, 3865 (1996).

[26] H. J. Monkhorst and J. D. Pack, Special points for Brillouin-zone integrations, Phys. Rev. B **13**, 5188 (1976).

[27] S. Grimme, Semiempirical GGA-type density functional constructed with a long-range dispersion correction, J. Comput. Chem. **27**, 1787 (2006).

[28] R. Fasel, P. Aebi, R. G. Agostino, D. Naumović, J. Osterwalder, A. Santaniello, L. Schlapbach, Orientation of Adsorbed C_{60} Molecules Determined Via X-Ray Photoelectron Diffraction, Phys. Rev. Lett. **76**, 4733 (1996).

[29] L.-L. Wang, H.-P. Cheng, Rotation, translation, charge transfer, and electronic structure of C_{60} on Cu(111) surface, Phys. Rev. B **69**, 045404 (2004).